Low-temperature drying of salted cod (*Gadus morhua*) assisted by high power ultrasound: kinetics and physical properties

César Ozuna[a], Juan A. Cárcel[a], Per M. Walde[b], Jose V. Garcia-Perez[a]

[a]Grupo de Análisis y Simulación de Procesos Agroalimentarios. Departamento de Tecnología de Alimentos. Universitat Politècnica de València. Camino de Vera. s/n. E46022. Valencia, Spain

[b]Aalesund University College, N-6025 Ålesund, Norway

*Corresponding author. Tel.: +34 96 387 93 76; Fax: +34 96 387 98 39

E-mail address:jogarpe4@tal.upv.es

ABSTRACT

Low-temperature convective drying could be considered an affordable alternative to conventional freeze-drying for foodstuffs. The process intensification should be based on non-thermal technologies, such as power ultrasound. Thereby, the aim of this work was to evaluate the air-borne application of power ultrasound on the low-temperature drying of salted cod. For that purpose, drying experiments were carried out at -10, 0, 10 and 20 °C on salted cod slabs at 2 m/s with (AIR+US, 20.5 kW/m^3) and without ultrasonic application (AIR). In the dried-salted cod, its rehydration capacity was analyzed, as were the microstructural, textural and color changes. At every temperature tested, ultrasound application increased the drying rate; thus, an average increase of 74% was observed in the effective diffusivity. AIR+US dried samples were softer and exhibited a higher rehydration capacity than AIR ones, which was linked to the microstructural changes produced by ultrasound. In addition, color changes were induced by ultrasound application.

Keywords: Ultrasonic; non-thermal processing, dehydration; microstructure; texture; color.

Introduction

Dried-salted cod (*Gadus morhua*) or klipfish has long been highly appreciated due to its high nutritional value and specific sensory properties (Walde, 2003). Although, dried-salted cod presents a water content of under 45% (wet basis), its salt content may reach 20% (wet basis) (Barat, Rodríguez-Barona, Andrés, & Fito, 2003). The processing includes the following steps: salting, washing, pre-drying by keeping the green salted cod for several days in piles outside the drying chambers, drying, grading and packaging (Oliveira, Pedro, Nunes, Costa, & Vaz-Pires, 2012). The drying of salted cod is performed at temperatures of around 20 ºC and at relative humidities of under 70% (Walde, 2003). Two main products can be found on the market depending on the intensity of the drying process: semi-dried or extra-dried cod.

The quality of dried-salted cod is greatly influenced by the salting and drying operation (Kilic, 2009). Salting induces changes in the muscle protein, generating modification in the texture, weight and water holding capacity (Oliveira et al., 2012). As far as drying is concerned, the use of high temperatures entails chemical and microbiological changes (Ortiz et al., 2013), structural, physical and mechanical modifications (Duan, Jiang, Wang, Yu, & Wang, 2011), crust formation on the surface (Bellagha, Sahli, Farhat, Kechaou, & Glenza, 2007) and the reduction of the hydration capacity of proteins (Brás & Costa 2010).

The use of low-temperature convective drying constitutes an interesting alternative means of improving the quality of the dried-salted cod due to the fact that it provides products with similar quality characteristics than conventional freeze-drying at lower cost (Kilic, 2009). The term “low temperature” makes reference to the use of air temperatures below standard room conditions, which includes figures below or close to the product’s freezing point. Despite its great potential, the use of low-temperatures in convective drying is mostly limited by the low drying rate, which retards the dehydration process and directly increases the processing costs (Walde, 2003). In this regard, it is of great interest to deal with the process intensification in order to improve the drying rate. For that purpose, coupling non-thermal technologies, such as power ultrasound (Ortuño, Martínez-Pastor, Mulet, & Benedito, 2012), to convective drying so as to achieve a higher yield, a lower energy use and high product quality and processing safety (Garcia-Perez, Carcel, Riera, Rosselló, & Mulet, 2012a) is worth exploring.

The application of power ultrasound may be accomplished by direct-contact or air-borne transmission (Schössler, Jäger, & Knorr, 2012a; Ozuna, Cárcel, García-Pérez, & Mulet, 2011). In direct-contact applications, there is an intimate contact between ultrasonic source and product, while in air-borne applications, ultrasound is transmitted through the air. Despite air-borne applications are less efficient than direct-contact ones in terms of energy yield, its lower heating effect and better adaptability to convective driers have largely contributed to its development. The feasibility of the ultrasonic application should be evaluated considering both kinetic and quality issues (Ozuna, Puig, García-Pérez, Mulet, & Cárcel, 2013; Vilkhua, Mawsona, Simonsa, & Bates, 2008).

Air-borne ultrasound applications have been reported to assist conventional hot-air drying (Ozuna et al., 2011; Garcia-Perez, Ortuño, Puig, Carcel, & Perez-Munuera, 2012b) and, more recently, for the convective freeze-drying (Bantle & Eikevik, 2011; Garcia-Perez et al., 2012a). Previous results have shown that air-borne ultrasound application during drying may greatly accelerate water removal. However, the effectiveness of ultrasound greatly depends on the process and product variables, such as temperature, air velocity, acoustic power applied, and product porosity (Cárcel, García-Pérez, Benedito, & Mulet, 2012). In addition, as far as we are concerned, the most recent air-borne applications have been focused on the drying of fruits and vegetables and few works have addressed the treatment of protein matrices, such as meat or fish products (Nakagawa, Yamashita, & Miura, 1996).

According to literature, ultrasound is able to produce modifications in food quality parameters such as texture, color, flavor and nutrients (Pingret, Fabiano-Tixier, & Chemat, 2013). To understand the effect of high power ultrasound on food quality, it is important to know the interactions between acoustic energy and the food structure (Jaeger, Reineke, Schoessler, & Knorr, 2012). Although several papers have focused on the quality changes brought about by ultrasonic applications in liquid media (Ahmad-Qasem et al., 2013 Wu, Hulbert, & Mount, 2000), few references have addressed this issue in gas media applications. In hot air drying and direct-contact ultrasonic application, Soria et al. (2010) and Schössler, Thomas, and Knorr (2012b) have studied the changes in chemical and physical quality parameters induced by a direct-contact ultrasonic application during the dehydration of carrot (20, 40 and 60 ºC, 1.2 m/s) and potato (70 ºC), respectively. Garcia-Perez et al. (2012b) and Puig, Perez-Munuera, Carcel, Hernando, and Garcia-Perez (2012) reported that the application of ultrasound during drying (40 ºC and 1 m/s) of orange peel and eggplant, respectively, could contribute to a better preservation of the quality (internal food structure) due to the shortening of the drying time. Schössler, Jager, and Knorr (2012c) reported that bulk density, color, ascorbic acid content and rehydration characteristics of red bell pepper was not affected by an ultrasonically (direct-contact) accelerated freeze-drying .

The main aim of this work was to evaluate the air-borne application of power ultrasound on the low-temperature drying of salted cod, quantifying its influence on the drying kinetics and on the physical properties of the final dried product.

2. Materials and methods

2.1. Raw material and shaping samples

Salted cod (*Gadus morhua*) was provided by a local supplier (Carmen Cambra S. L., Spain), to better ensure the homogeneity of the raw material. According to supplier specifications, cod fish were caught in high seas and processed immediately in the fishing boat (bled, gutted, beheaded, split and salted). On average, the pieces of salted cod weighed 1.5±0.25 kg.

Parallelepiped-shaped samples (length 50 mm, width 30 mm and thickness 10 mm) were obtained from the central part of the salted cod loin using a sharp knife. The samples were wrapped in plastic waterproof film and stored at -18 ± 0.5 ºC until the drying experiments were carried out (maximum storage time 120 h). The initial moisture and the NaCl content were measured following standard methods 950.46 and 971.27, respectively (AOAC, 1997).

2.2. Drying experiments

The drying experiments of salted cod slabs were conducted in a convective drier with air recirculation and temperature and air velocity control. Air temperature and velocity are controlled using a PID algorithm. A cooper tube heat exchanger (Frimetal, Spain), installed in the air duct, cooled down the air to temperatures close to -20 ºC, which was subsequently heated using electrical devices (3000 W). The air temperature and relative humidity were measured at three points in the air duct using a combined sensor (KDK, Galltec+Mela, Germany).

The drier includes an ultrasonically activated drying chamber, already described in literature (Garcia-Perez et al., 2012a). The air-borne ultrasound application system consisted of a cylindrical radiator (internal diameter 100 mm, height 310 mm, thickness 10 mm) driven by a power ultrasonic transducer (frequency 21.9 kHz, impedance 369 Ω, power capacity 90 W). The ultrasonic system provided an average sound pressure level in the drying chamber of 155 dB. A resonance dynamic controller was connected to a PC by the RS-232 interface to adequately monitor the main electric parameters of the system during the air-borne ultrasonic application (power, intensity, voltage, phase, frequency and impedance).

The cod samples were weighed at preset times using an industrial weighing module (6000±0.01 g; VM6002-W22, Mettler-Toledo, USA). An application was developed using LabVIEW 2011 programming code (National Instruments, USA) to provide overall control and monitoring of the ultrasonically intensified drying process, integrating information on the air flow, the sample and the ultrasonic parameters.

Air-drying (AIR) and ultrasonically assisted air-drying (AIR+US) experiments were conducted at -10, 0, 10 and 20 ± 1 °C, 2 ± 0.1 m/s and an average relative humidity of 9 ± 4%. In the AIR+US experiments, an acoustic power density of 20.5 kW/m^3 was applied (Ozuna et al., 2011). Prior to the drying experiments, the sealed samples (9 slabs per experiment) were tempered at the drying temperature for 24 h. Then, the cod slabs were unwrapped and placed on the sample holder, which consists of a metallic frame where samples are suspended to allow free airflow around the slabs, and introduced into the drying chamber. The sample weight was automatically measured and recorded at regular time intervals (15 min). The drying experiments were replicated at least three times for each condition tested and extended until the samples lost 20% of the initial weight, which is a usual figure for klipfish (Oliveira et al., 2012).

2.3. Rehydration experiments

Rehydration experiments of dried-salted cod (AIR and AIR+US at -10, 0, 10 and 20 °C) were carried out by immersing the samples in distilled water at 4 ± 1 ºC for 27 h. The ratio of cod and water volume was kept as 1:20. In this study, the rehydration kinetics were studied globally from the evolution of the net sample weight that includes both moisture and salt transport, since samples both gained water and lost salt. For that purpose, samples were taken at regular time intervals, superficially drained with absorbent paper to remove surface water and weighed. Thus, the net weight change was monitored (Eq. (1)).

$$\Delta M^{0}{}_{t} = \frac{M_t - M_0}{M_0} \qquad (1)$$

For each drying condition tested, a minimum of 6 rehydration experiments were carried out.

2.4. Modeling

2.4.1 Drying

A diffusion model, based on Fick's law, was used to mathematically describe the drying kinetics (AIR and AIR+US) of cod samples. The differential equation of diffusion is obtained by combining Fick's law and the microscopic mass balance. For infinite slab geometry, the diffusion equation is shown in Eq. (2), assuming the effective moisture diffusivity as constant and the solid to be isotropic.

$$\frac{\partial W_p(x,t)}{\partial t} = D_W \left(\frac{\partial^2 W_p(x,t)}{\partial x^2} \right) \qquad (2)$$

In order to solve Eq. (2), some further assumptions were considered: solid symmetry, a uniform initial moisture content and temperature, constant shape during drying and a negligible external resistance to water transfer. Taking these assumptions into account, the analytical solution of the diffusion equation is expressed in terms of the average moisture content in Eq. (3) (Crank, 1975).

$$W = W_{eq} + (W_0 - W_{eq})\left[2\sum_{n=0}^{\infty}\frac{1}{\lambda_n^2 L^2}e^{-D_W \lambda_n^2 t}\right] \quad (3)$$

where, λ_n are the eigenvalues calculated as $\lambda_n L = (2n+1)\frac{\pi}{2}$

The equilibrium moisture data were obtained from the desorption data of salted cod at 25 ºC reported by Walde (2003).

2.4.2 Rehydration

The evolution of sample weight during rehydration was modeled by means of Peleg's empirical equation (Peleg, 1988) (Eq. (4)).

$$M_t = M_0 + \frac{t}{k_1 + k_2 t} \quad (4)$$

where $1/k_1$ and $1/k_2$ are the model's parameters. The rate constant, $1/k_1$, is related to the weight gain rate at the very beginning, $t = t_0$, and represents the initial rehydration rate (Eq. (5)).

$$\frac{dM\left(t = t_0\right)}{dt} = \frac{1}{k_1} \quad (5)$$

The capacity constant, $1/k_2$, is related to the equilibrium weight (M_e). Thus, when rehydration time is very long, Eq. (4) becomes Eq. (6), giving the relationship between M_e and $1/k_2$.

$$M_e = M_0 + \frac{1}{k_2} \quad (6)$$

2.4.3 Model fitting

The model parameters (D_W of diffusion model and $1/k_1$ and $1/k_2$ of Peleg model) were identified by using an optimization procedure that minimized the sum of the squared differences between the experimental and calculated average data. For that purpose, the non-linear optimization algorithm of the Generalized Reduced Gradient (GRG), available in Microsoft Excel™ spreadsheet from MS Office 2010 (Microsoft Corp., USA), was used. The goodness of the fit was determined by the percentage of explained variance, %VAR (Eq. (7)).

$$\%VAR = \left[1 - \frac{S_{xy}^2}{S_y^2}\right] \cdot 100 \qquad (7)$$

2.5. Texture

Hardness, characterized as the maximum penetration force, was evaluated in the dried and rehydrated samples using a Texture Analyzer (TAX-T2®, Stable Micro System, United Kingdom). Penetration tests were conducted with a 2 mm flat cylinder probe (SMS P/2N), at a crosshead speed of 1 mm/s and a strain of 70% (penetration distance 7 mm). In each sample, penetration tests were carried out at 12 points following a preset pattern.

2.6. Microstructure. Scanning Electron Microscopy (SEM)

Cubes (side 3 mm) from samples dried at 0 ºC with and without ultrasound application were immersed in liquid N_2 and then freeze-dried at 1 Pa for 3 days (LIOALFA-6, Telstar, Spain). Then, samples were vacuum sealed in vials in the same freeze-drier, so that they would remain stable (Ozuna et al., 2013). After that, they were individually placed on SEM slides with the aid of colloidal silver and then gold-coated with carbon (SCD005, Baltec, Germany) at 10^{-2} Pa and an ionization current of 40 mA. The samples were observed in a scanning electron microscope (JSM-5410, Jeol, Japan) equipped with a LINK data-processing system (INCA 4.09, Oxford Instruments, England) at an acceleration voltage of 10-20 kV.

2.7. Color

The color of dried-salted cod was measured by computing the CIE L*a*b* color coordinates using a colorimeter (Minolta CR-200, Konica Minolta Optics, Inc., Japan). In each slice, color test was conducted at 6 points following a preset pattern. According to CIE L*a*b* system, L^* measures the lightness on a 0 to 100 scale from black to white; a^*, (+) red or (-) green; and b^*, (+) yellow or (-) blue (Bai, Sun, Xiao, Mujumdar, & Gao, 2013). The overall color differences (ΔE) between AIR and AIR+US samples were also determined by Eq. (8).

$$\Delta E = \sqrt{\Delta L^{*2} + \Delta a^{*2} + \Delta b^{*2}} \quad (8)$$

2.8. Statistical analysis

In order to identify whether ultrasound and the air temperature significantly ($p<0.05$) influenced the drying, rehydration properties and the texture and color of dried-salted cod, analysis of variance (ANOVA) ($p<0.05$) was carried out and the least significant difference (LSD) intervals were identified using the Statgraphics Plus 5.1. statistical package (Statistical Graphics Corp., USA).

3. Results and discussion

3.1 Experimental drying kinetics

The experimental drying kinetics (AIR, AIR+US) of salted cod slabs at -10, 0, 10 and 20 ºC are shown in Fig. 1. The average initial moisture and NaCl contents of salted cod were 1.23±0.07 kg W/kg dry matter and 0.41±0.03 kg NaCl/kg dry matter, respectively. Both the fact that the raw matter used constitutes a partially-dried material and also the high concentration of NaCl in cod flesh limits the presence of free water. For this reason, no constant rate drying period was observed and drying occurred in the falling rate period (Bellagha et al., 2007). Thus, the initial moisture content was considered as the critical one for modeling purposes.

As stated in Section 2.2, drying experiments were extended until the weight loss reached 20% of the initial weight. Thereby, dried-salted samples presented final moisture and NaCl contents of 0.77±0.04 kg W/kg dry matter and 0.41±0.02 kg NaCl/kg dry matter, respectively. The results obtained for the AIR experiments showed that the air temperature affected drying kinetics, shortening the drying time. For example, the drying time for the lowest temperature tested, -10 ºC, was over 14 h, while at 20 ºC, it was only 5 h. Air temperature was found to have a similar influence in AIR+US experiments.

The application of power ultrasound sped up the drying kinetics, as can be observed if the AIR and AIR+US experiments are compared (Fig. 1). Ultrasound application led to a shortening of the drying time of between 35 and 54% as compared to AIR experiments. The greatest time reduction under ultrasound application was found at the lowest and the highest temperatures tested (-10 and 20 ºC). Using the same ultrasonic set-up and under similar experimental conditions, Garcia-Perez et al. (2012a) found drying time reductions of 68 and 70% in the drying of carrot and eggplant cubes (-14 ºC and 2 m/s), respectively.

When drying green peas at -3 ºC, Bantle and Eikevik (2011) showed that, with ultrasound application (20 kHz; DN 20/2000, Sonotronic), there was a maximum reduction in the drying time of around 10%. On the other hand, drying surimi slabs at 20 ºC and 2.8 m/s, Nakagawa et al. (1996) observed that the drying time was 80% shorter when acoustic waves (155.5 dB, 19.5 kHz) were applied.

3.2 Modeling drying kinetics

In order to quantify the influence of power ultrasound application and temperature on the drying kinetics of salted cod slabs, the proposed diffusion model (Eq. (3)) was fitted to the experimental data.

The diffusion model provided a percentage of explained variance (%VAR) close to 99% for AIR and AIR+US experiments at 0, 10 and 20 ºC (Table 1). This fact suggests that, in these cases, the drying process followed a clear diffusion pattern. In the case of AIR+US experiments at -10 ºC, the explained variance achieved by the model was much lower (95.4%) than at other temperatures, and also lower than that found in AIR experiments at the same temperature (98.3%). This indicates that there is some influence of ultrasound on the mass transfer control mechanisms and diffusion was not the only significant mechanism controlling water transport. In this regard, Garcia-Perez et al., (2012a) observed the same behavior when analyzing the low-temperature drying (-14 ºC, 2 m/s) of carrot and highlighted that, under such particular conditions, ultrasound application led to a larger improvement in the diffusion coefficient (407-428%) than it did in the mass transfer coefficient (96-170%). Therefore, the application of power ultrasound reduced the internal resistance to mass transfer more than the external, which means that diffusion does not prevail as the most significant ($p<0.05$) water transfer controlling mechanism and convection grows in importance.

In AIR experiments, D_W values ranged from 0.14 x 10^{-10} to 0.35 x 10^{-10} m^2/s. Temperature affected the effective moisture diffusivity, so, the higher the temperature applied, the greater the identified effective moisture diffusivity (Table 1). The effective moisture diffusivities identified for the AIR experiments are close to other reported values. Park (1998) obtained values of around 0.87-1.61 x 10^{-10} m^2/s for salted fish muscle dried at 20-40 ºC. In a data compilation of the moisture diffusivity of foodstuffs, Zogzas, Maroulis, and Marinos-Kouris (1996) reported D_W values ranging between 0.13 x 10^{-10} and 3.1 x 10^{-10} m^2/s for the drying of unsalted fish muscle (30 ºC).

The application of high power ultrasound significantly increased ($p<0.05$) the effective moisture diffusivity at every temperature tested. The increase in this parameter (ΔD_W) ranged from 110% at the highest temperature tested, 20 ºC, to 42% at 0 ºC (Table 1). The improvement in the D_W values is mainly linked with the mechanical effects brought about by applying ultrasound to the material being dried (Puig et al., 2012). Ultrasound introduces a series of rapid and cyclic compressions and expansions of the material that can be compared to a sponge being squeezed and released repeatedly, thus improving the water diffusion in the particle. Moreover, acoustic energy also introduces pressure variations, oscillating velocities, and microstreaming on the solid-gas interfaces, reducing boundary layer thickness and, therefore, improving the water transfer rate from the solid surface to the air medium (Cárcel et al., 2012).

The influence of air temperature on D_W identified for AIR and AIR+US experiments followed an Arrhenius type relationship (Fig. 2) (Bai et al., 2013). A similar activation energy of 20.46 and 21.79 kJ/mol was obtained for AIR and AIR+US drying experiments, respectively. In such a way, the energy needed for water removal was not affected by ultrasound application. The activation energy figures are similar to those proposed by other authors for fish drying. Thus, Jason (1958) reported an activation energy of 30 kJ/mol for cod muscle (unsalted) and Park (1998) a value of 21.94 kJ/mol for the drying of salted shark muscle.

From Fig. 2, the D_W values for AIR and AIR+US experiments are easily compared. It may be observed that the D_W for AIR+US experiments at -10 ºC was similar to the figure found in AIR experiments at 0 ºC. Similar values were also found for AIR+US and AIR experiments at 0 and 20 ºC, respectively. This fact suggests that the increase in D_W produced by US application could be equivalent to a temperature rise of between 10 and 20 ºC.

3.3. Rehydration kinetics

Samples dried under the different conditions tested were rehydrated in distilled water at 4 ºC. The net weight change was used to monitor the process kinetics (ΔM^0_t), in which a coupled water and salt transfer exists. The experimental data showed that the drying air temperature influenced the rehydration kinetics (Fig. 3). For example, after 27 h of rehydration, AIR samples dried at 20 ºC gained 38% more weight than that observed in samples dried at -10 °C. Duan et al. (2011) reported that the rehydration ratio of dried tilapia fish fillets increased with the rise in drying temperature. Likewise, Russo, Adiletta, and Di Matteo. (2013) connected the drying temperature with a marked influence on the microstructure of dried products; high drying temperatures led to an increase in porosity and the collapse of the structure, causing a rise in the initial water uptake during rehydration.

The application of ultrasound during drying affected the rehydration ability of dried-salted cod samples. The AIR+US samples exhibited a higher final weight gain than AIR ones (Fig. 3) and, therefore, a higher final water content (Table 2). As regards the final NaCl content, no significant ($p>0.05$) changes were observed between AIR and AIR+US samples.

The higher water gain in AIR+US dried samples could be linked to changes produced by ultrasound in the microstructure during drying (Fig. 4). According to the SEM micrograph obtained from the longitudinal section of salted cod dried at 0 ºC, AIR+US samples (Figs. 4 D and E) showed a more damaged and collapsed structure than AIR ones (Figs. 4 A and B). Ultrasound application provoked ruptures in the cod fibers (Fig 4 E) and a greater migration of salt to the fiber surface (Fig. 4 D). In addition, micrographs obtained from a cross section of AIR+US dried-salted cod exhibited the formation of wider spaces between myofibrils and a more intense salt redistribution on the surface (Fig. 4 F). Hence, these structural differences which are induced by mechanical effects linked to ultrasound can explain the greater weight gain of AIR+US samples during rehydration. In addition, the fact that ultrasound application leads to a shorter drying time can lessen the damage to the protein structure (denaturation), contributing to a greater water holding capacity, thereby increasing the rehydration capacity of AIR+US samples (Brás & Costa, 2010).

3.4. Modeling rehydration kinetics.

The Peleg model was used to analyze and quantify the influence of both drying temperature and ultrasound application on the net weight gain (ΔM^0_t) of dried-salted cod slabs during rehydration. As can be observed in Table 3, the model adequately described the rehydration kinetics, providing percentages of explained variance ranging between 96.8 and 99.3%.

The identified Peleg parameters, related to the initial mass transfer rate ($1/k_1$) and the equilibrium weight ($1/k_2$), are shown in Table 3. As far as the effect of the drying temperature is concerned, the identified model parameters for AIR samples slightly increased when the temperature rose (Table 3). However, these increases were only significant ($p<0.05$) for the equilibrium constant, $1/k_2$. Air temperature was also observed to have a similar effect on AIR+US samples.

The application of ultrasound during drying significantly modified ($p<0.05$) the Peleg parameters at every drying air temperature tested. There was a faster and more substantial rehydration of AIR+US samples than AIR samples, which could be observed in the increase in both $1/k_1$ and $1/k_2$ parameters. Thereby, when comparing the rehydration patterns of AIR and AIR+US samples, the changes observed should be related to the structural changes brought about by ultrasound and depicted in Section 3.3. As can be observed in Table 3, ultrasound had a greater effect on Peleg parameters, $\Delta 1/k_1$ and $\Delta 1/k_2$, at the lowest temperatures tested (-10 and 0 ºC) than at the highest ones (10 and 20 ºC). This fact could be linked to the length of time samples are exposed to the ultrasonic energy. While drying experiments carried out at the lowest temperatures (-10 and 0 ºC) lasted approximately 6 to 8 h, at the highest temperatures (10 and 20 ºC), the drying time was reduced by almost half (Fig. 1). Therefore, the longer the exposure time to ultrasound application, the more intense the ultrasound effects on the cod structure (Fig. 4).

3.5. Texture

The hardness of dried and rehydrated cod was evaluated by computing the maximum penetration force. The initial hardness value of salted cod was 3.62 ± 0.35 N, thus, the drying process provoked a hardening of the samples (Table 4). The measurements taken from AIR samples showed that the sample hardness was dependent on the drying air temperature used (Table 4); the higher the air temperature applied, the harder the dried cod. Thus, AIR samples dried at 10 and 20 °C were significantly ($p<0.05$) harder than those dried at 0 and -10 °C. The temperature rise could induce a greater denaturation of the connective tissues and the myofibrillar proteins (myosin and actin) promoted by NaCl, leading to the sample hardening. (Ortiz et al., 2013; Brás & Costa, 2010).

As is shown in Table 4, AIR+US dried samples were significantly ($p<0.05$) softer than AIR ones. This fact could be linked to the mechanical effects caused by ultrasound application on salted cod fibers (Figs. 4 D, E and F). The fact that the structure of the AIR+US samples is more collapsed and porous than the AIR samples (Figs. 4 A, B and C) explains the low degree of hardness found. In addition, the application of ultrasound is linked to a reduction in the drying time which could contribute to some mild damage in the protein structure, causing a lesser degree of hardening (Oliveira et al., 2012; Kilic, 2009). Moreover, the hardness of AIR+US samples was not affected by the drying air temperature (Table 4).

The hardness was also measured in rehydrated samples (4 ºC, 27 h). As can be observed in Table 4, the rehydration produced a softening of dried-salted samples. After rehydration, AIR samples dried at -10, 10 and 0 ºC were significantly ($p<0.05$) softer than those dried at 20 ºC. This fact suggests that drying at 20 ºC affected the structure of the dry material, limiting the softening of rehydrated samples. At every temperature tested, AIR+US rehydrated samples were softer than AIR ones, which is consistent with the effect observed in rehydration kinetics (Fig. 3, Table 2) produced by structural changes (Fig. 4).

3.6. Color

The color of dried-salted cod is generally considered to be one of the most relevant quality traits. In order to analyze the influence of ultrasound application and drying temperature on the color changes of dried-salted cod, CIE L*a*b* color coordinates were measured directly on dried samples under different conditions (AIR and AIR+US at -10, 0, 10 and 20 ºC). The average values of chromatic coordinates (L*, a*, b*) for raw salted cod were L*=58.93±2.00, a*=-3.66±0.49 and b*=4.86±1.50. Thus, as observed in Fig. 5, the drying process provoked changes in the color of fish muscle (Fig.5). In general terms, L*, a* and b* increased, which indicates that the drying process caused both the yellowing (higher b*) of the samples and the increase in their lightness index (higher L*) (Brás & Costa, 2010, Lauritzsen et al., 2004).

In AIR samples, L* and b* coordinates values were significantly ($p<0.05$) affected by the drying air temperature; the higher the temperature applied, the lower the values of L* and b* (Figs. 5 A, C). This may be explained by the fact that a temperature rise induces, in the cod muscle, the contraction of myotomes due to protein aggregation (Fernandez-Segovia, Camacho, Martinez-Navarrete, Escriche, & Chiralt, 2003), the oxidation of phospholipids and reactions which stem from the presence of other ions in the salt composition (Oliveira et al., 2012). This leads to an increase in the opacity of the fish tissue (Lauritzsen et al., 2004) and contributes to the color degradation of dried-salted cod samples. The experimental measurements obtained coincide with those reported by Ortiz et al. (2013), who studied the influence of drying air temperature on the color of dried salmon (*Salmo salar* L.) fillets and found a significant ($p<0.05$) decrease in L* and b* values when comparing samples dried at 40 and 60 ºC. On the contrary, the a* value for AIR samples did not show any significant ($p<0.05$) temperature-linked trend (Fig. 5 B).

As observed in Figure 5 D, there were found to be changes between the color (ΔE) of AIR+US and AIR samples, which were dependent on the drying temperature (Fig. 5 D); thus, the lower the drying temperature, the greater the color differences between AIR and AIR+US samples. These differences are obviously linked to specific changes in chromatic coordinates (L*, b* and a*), although no common pattern was found. As regards L* and b* coordinates, AIR+US samples dried at -10 and 0 ºC exhibited higher lightness (L*) and lower yellowness (b*) values in comparison to AIR samples, which could be interesting for the cod industry which requires products with high whiteness values (Oliveira et al., 2012). Moreover, AIR+US samples dried at 10 and 20 ºC did not show significant ($p<0.05$) changes in L* and b* coordinates compared to AIR samples (Figs. 5 A, C). According to the a* coordinate (Fig. 5 B), there was a significant ($p<0.05$) effect of ultrasound on samples dried at -10, 0 and 10 ºC; however, this effect did not exhibit a significant temperature-linked trend.

4. Conclusions

The application of power ultrasound during the drying of salted cod improved the drying rate, shortening the drying time by an average of 35-50%. Water removal at 0, 10 and 20 ºC showed a diffusion pattern, while at -10 ºC convection was also significant, especially when ultrasound was applied. Microstructural analyses showed that the application of ultrasound during drying brought about changes in cod fibers, which led to a higher rehydration capacity and softer samples. Ultrasound also promoted changes in dried-salted cod, particularly an increase in lightness (L*) at low temperatures. Therefore, the feasibility of power ultrasound, a non-thermal technology, to improve the low-temperature drying of salted cod has been highlighted and further studies should address whether the kinetic improvement is coupled to an energy reduction, which could bring this technology closer to a potential industrial use.

ACKNOWLEDGMENTS

The authors acknowledge the financial support both from the Ministerio de Economía y Competitividad (Ref. DPI2012-37466-C03-03) and Carmen Cambra S.L. for their technical support with the selection of the raw material. César Ozuna was the recipient of a fellowship from the Universitat Politècnica de València for his research stay in Aalesund University College.

NOMENCLATURE

D_W	Effective moisture diffusivity, m^2/s
ΔD_W	Increase in effective moisture diffusivity produced by ultrasound application, %
L	Half thickness, m
x	Characteristic coordinate in slab geometry, m
λ_n	Eigenvalues
S_y	Standard deviation of the sample
S_{yx}	Standard deviation of the estimation
t	Time, s
M_0	Initial weight, g
M_t	Weight at time t, g
M_e	Equilibrium weight, g
ΔM^0_t	Net weight change, g
W	Average moisture content, kg water/kg dry matter
W_0	Initial moisture content, kg water/kg dry matter
W_p	Local moisture content, kg water/kg dry matter
W_{eq}	Equilibrium moisture content, kg water/kg dry matter
$1/k_1$	Peleg rate constant, g water/g dry matter × s
$1/k_2$	Peleg capacity constant, g
$\Delta 1/k_1$	Increase in Peleg rate constant produced by ultrasound application, %
$\Delta 1/k_2$	Increase in Peleg capacity constant produced by ultrasound application, %
L*	Chromatic coordinate, lightness 0 (black) to 100 (white)

a*	Chromatic coordinate, (+) red or (-) green
b*	Chromatic coordinate, (+) yellow or (-) blue

References

Ahmad-Qasem, M. H., Cánovas, J., Barrajón-Catalán, E., Micol, V., Cárcel, J. A., & García-Pérez, J. V. (2013). Kinetic and compositional study of phenolic extraction from olive leaves (var. Serrana) by using power ultrasound. *Innovative Food Science & Emerging Technologies*, 17, 120-129.

AOAC. (1997). *Official Methods of Analysis*. Association of Official Analytical Chemists: (Virginia, USA).

Bai, J.-W., Sun, D.-W., Xiao, H.-W., Mujumdar, A.S., & Gao, Z.-J. (2013). Novel high-humidity hot air impingement blanching (HHAIB) pretreatment enhances drying kinetics and color attributes of seedless grapes. *Innovative Food Science & Emerging Technologies*, in press, DOI: 10.1016/j.ifset.2013.08.011.

Bantle, JM., & Eikevik, T. M. (2011). Parametric study of high-intensity ultrasound in the atmospheric freeze drying of peas. *Drying Technology*, 29, 1230-1239.

Barat, J.M., Rodriguez-Barona, S., Andrés, A., & Fito, P. (2003). Cod salting manufacturing analysis. *Food Research International*, 36, 447-453.

Bellagha, S., Sahli, A., Farhat, A., Kechaou, N., & Glenza, A. (2007). Studies on salting and drying sardine (*Sardinella aurita*): Experimental kinetics and modeling. *Journal of Food Engineering*, 78, 947-952.

Brás, A., & Costa, R. (2010). Influence of brine salting prior to pickle salting in the manufacturing of various salted-dried fish species. *Journal of Food Engineering*, 100, 490–495.

Cárcel, J.A., García-Pérez, J.V., Benedito, J., & Mulet, A. (2012). Food process innovation through new technologies: use of ultrasound. *Journal of Food Engineering*, 110, 200-207.

Crank, J. (1975). *The mathematics of diffusion*. Oxford university press.

Duan, Z., Jiang, L., Wang, J., Yu, X., & Wang, T. (2011). Drying and quality characteristics of tilapia fish fillets dried with hot air-microwave heating. *Food and Bioproducts Processing*, 89, 472-476.

Fernandez-Segovia, I., Camacho, M.M., Martinez-Navarrete, N., Escriche, I., & Chiralt, A. (2003). Structure and color changes due to thermal treatments in desalted cod. *Journal of Food Processing Preservation*, 27, 465-474.

Garcia-Perez, J.V., Carcel, J.A., Riera, E., Rosselló, C., & Mulet, A. (2012a). Intensification of low-temperature drying by using ultrasound. *Drying Technology*, 30, 1199-1208.

Garcia-Perez, J.V., Ortuño, C., Puig, A., Carcel J.A., & Perez-Munuera, I. (2012b). Enhancement of water transport and microstructural changes induced by high-intensity ultrasound application on orange peel drying. *Food and Bioprocess Technology*, 5, 2256-2265.

Jaeger, H., Reineke, K., Schoessler, K., & Knorr, D. (2012). Effects of emerging processing technologies on food material properties. In B.R. Bhandari, & Y.H. Roos (Eds), *Food Materials Science and Engineering*, (pp. 222-254). Blackbell Publishing Ltd.

Jason, A.C. (1958). A study of evaporation and diffusion processes in the drying of fish muscle. In *Fundamental Aspects of the Dehydration of Foodstuffs* (pp. 103-155). Aberdeen: The Society of Chemical Industry.

Kilic, A. (2009). Low temperature and high velocity (LTHV) application in drying: characteristics and effects on the fish quality. *Journal of Food Engineering*, 91, 173-182.

Lauritzsen, K., Akse, L., Johansen, A., Joensen, S., Sørensen, N.K., & Olsen, RL. (2004). Physical and quality attributes of salted cod (*Gadus morhua L.*) as affected by the state of rigor and freezing prior to salting. *Food Research International*, 37, 677–688.

Nakagawa S., Yamashita T., & Miura H. (1996). Ultrasonic drying of walleye pollack surimi. *Journal of the Japanese Society for Food Science and Technology*, 43, 388-394.

Oliveira, H., Pedro S., Nunes, M.L., Costa, R., & Vaz-Pires, P. (2012). Processing of salted cod (*Gadus* spp.): a review. *Comprehensive Reviews in Food Science and Food Safety*, 11, 546-564.

Ortiz, J., Lemus-Mondaca, R., Vega-Gálvez, A., Ah-Hen, K., Puente-Diaz, L., Zura-Bravo, L., & Aubourg, S. (2013). Influence of air-drying temperature on drying kinetics, colour, firmness, and biochemical characteristics of Atlantic salmon (*Salmo salar* L.) fillets. *Food Chemistry*, 139, 162-169.

Ortuño, C., Martínez-Pastor, M. T., Mulet, A., & Benedito, J. (2012). An ultrasound-enhanced system for microbial inactivation using supercritical carbon dioxide. *Innovative Food Science & Emerging Technologies*, 15, 31-37.

Ozuna, C., Puig, A., García-Pérez, J.V., Mulet, A., & Cárcel, J.A. (2013). Influence of high intensity ultrasound application on mass transport, microstructure and textural properties of pork meat (*Longissimus dorsi*) brined at different NaCl concentrations. *Journal of Food Engineering*, 119, 84-93.

Ozuna, C., Cárcel, J.A., García-Pérez, J.V., & Mulet, A. (2011). Improvement of water transport mechanisms during potato drying by applying ultrasound. *Journal of the Science of Food and Agriculture*, 91, 2511–2517.

Park, K.J. (1998). Diffusional model with and without shrinkage during salted fish muscle drying. *Drying Technology*, 16, 889-905.

Peleg, M. (1988). An empirical model for the description of moisture sorption curves. *Journal of Food Science*, 53, 1216-1217.

Pingret, D., Fabiano-Tixier, A. S., & Chemat, F. (2013). Degradation during application of ultrasound in food processing: a review. *Food Control*, 31, 593-606.

Puig, A., Perez-Munuera, I., Carcel, J.A., Hernando, I., & Garcia-Perez, J.V. (2012). Moisture loss kinetics and microstructural changes in eggplant (*Solanum melongena L*.) during conventional and ultrasonically assisted convective drying. *Food and Bioproducts Processing*, 90, 624-632.

Russo, P., Adiletta, G., & Di Matteo, M. (2013). The influence of drying air temperature on the physical properties of dried and rehydrated eggplant. *Food and Bioproducts Processing*, 91, 249-256.

Schössler, K., Jäger, H., & Knorr, D. (2012a). Effect of continuous and intermittent ultrasound on drying time and effective diffusivity during convective drying of apple and red bell pepper. *Journal of Food Engineering*, 108, 103-110.

Schössler, K., Thomas, T., Knorr, D. (2012b). Modification of cell structure and mass transfer in potato tissue by contact ultrasound. *Food Research International*, 49, 425-431.

Schössler, K., Jager, H., Knorr, D. (2012c). Novel contact ultrasound system for the accelerated freeze-drying of vegetables. *Innovative Food Science and Emerging Technologies*, 16, 113-120.

Soria, A.C., Corzo-Martinez, M., Montilla, A., Riera, E., Gamboa-Santos, J., & Villamiel, M. (2010). Chemical and physicochemical quality parameters in carrots dehydrated by power ultrasound. *Journal of Agricultural and Food Chemistry*, 58, 7715-7722.

Vilkhu, K., Mawson, R., Simons, L., & Bates, D. (2008). Applications and opportunities for ultrasound assisted extraction in the food industry-A review. *Innovative Food Science & Emerging Technologies*, 9, 161-169.

Walde, P. M. (2003). *Transport Phenomena in Dehydration of Fish Muscle* (Doctoral dissertation, Norwegian University of Science and Technology).

Wu, H., Hulbert, G. J., & Mount, J. R. (2000). Effects of ultrasound on milk homogenization and fermentation with yogurt starter. *Innovative Food Science & Emerging Technologies*, 1, 211-218.

Zogzas, N. P., Maroulis, Z. B., & Marinos-Kouris, D. (1996). Moisture diffusivity data compilation in foodstuffs. *Drying technology*, 14, 2225-2253.

Figure captions

Figure 1. Drying kinetics of salted cod slabs (length 50 mm, width 30 mm and thickness 10 mm) at -10, 0, 10 and 20 ºC (2 m/s) with (AIR+US, 20.5 kW/m^3) and without (AIR) ultrasound application.

Figure 2. Influence of drying air temperature on the average effective moisture diffusivities identified for salted cod drying with (AIR+US, 20.5 kW/m^3) and without (AIR) ultrasound application.

Figure 3. Rehydration kinetics (4 °C) of salted cod slabs (length 50 mm, width 30 mm and thickness 10 mm) dried at -10, 0, 10 and 20 ºC (2 m/s) with (AIR+US, 20.5 kW/m^3) and without (AIR) ultrasound application.

Figure 4. Longitudinal and cross-section (x100) observed by SEM. Dried salted cod at 0 °C and 2 m/s with (AIR+US, 20.5 kW/m^3: D, E and F) and without ultrasound application (AIR: A, B and C).

Figure 5. CIELAB coordinates (L*, a*, b*) of salted cod (length 50 mm x width 30 mm x thickness 10 mm) dried at -10, 0, 10 and 20 ºC with (20.5 kW/m^3, AIR+US) and without (AIR) ultrasound application. ΔE represents the overall color change between AIR+US and AIR samples. Average values ± LSD intervals at a confidence level of 95% are plotted.

Figure 1

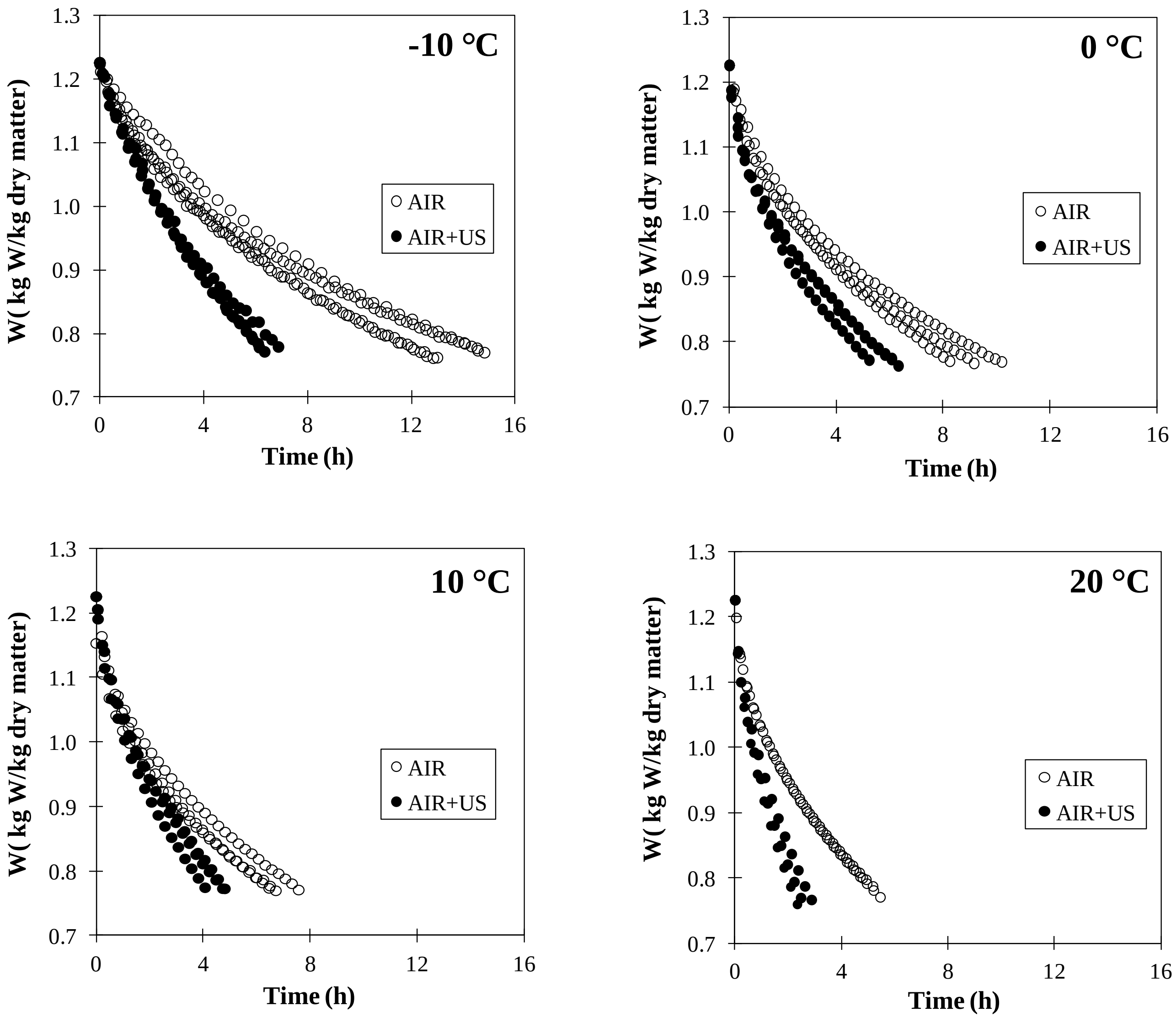

Figure 2

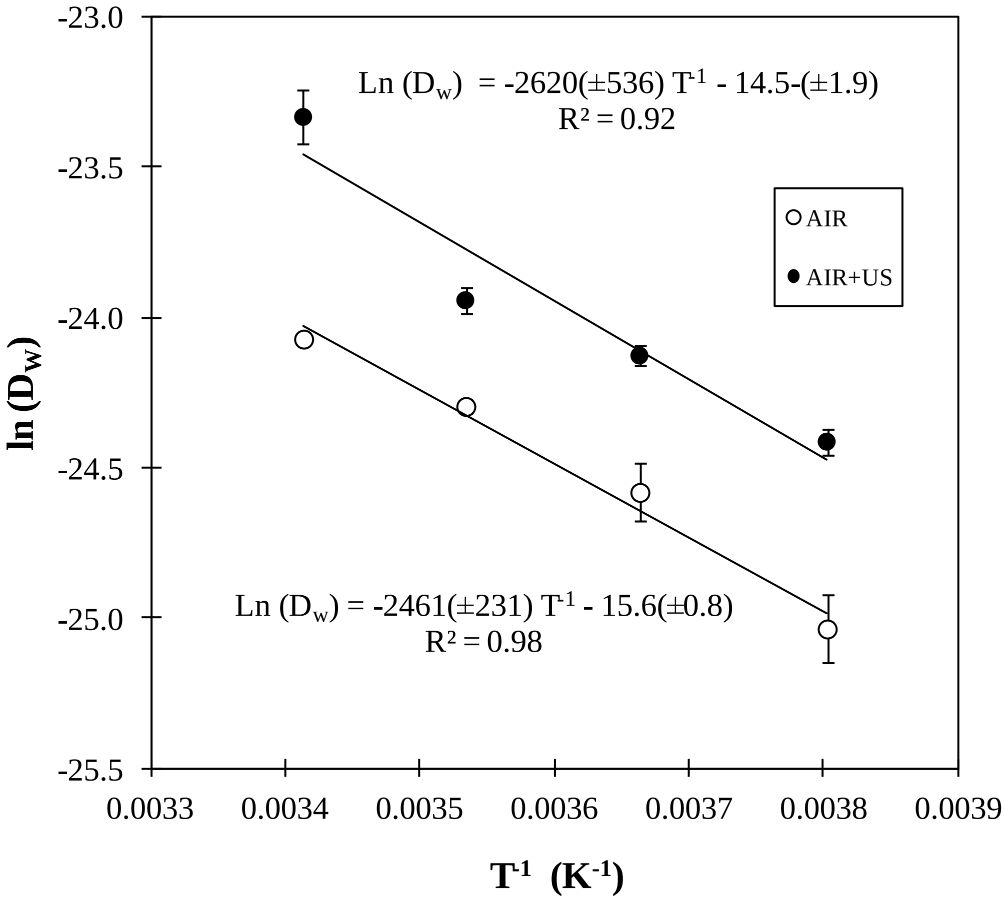

-23.0
-23.5
-24.0
-24.5
-25.0
-25.5
0.0033
0.0034
0.0035
0.0036
0.0037
0.0038
0.0039
ln (D$_W$)
T^{-1} (K^{-1})
Ln (D$_w$) = -2620(±536) T^{-1} - 14.5-(±1.9)
R² = 0.92
Ln (D$_w$) = -2461(±231) T^{-1} - 15.6(±0.8)
R² = 0.98
AIR
AIR+US

Figure 3

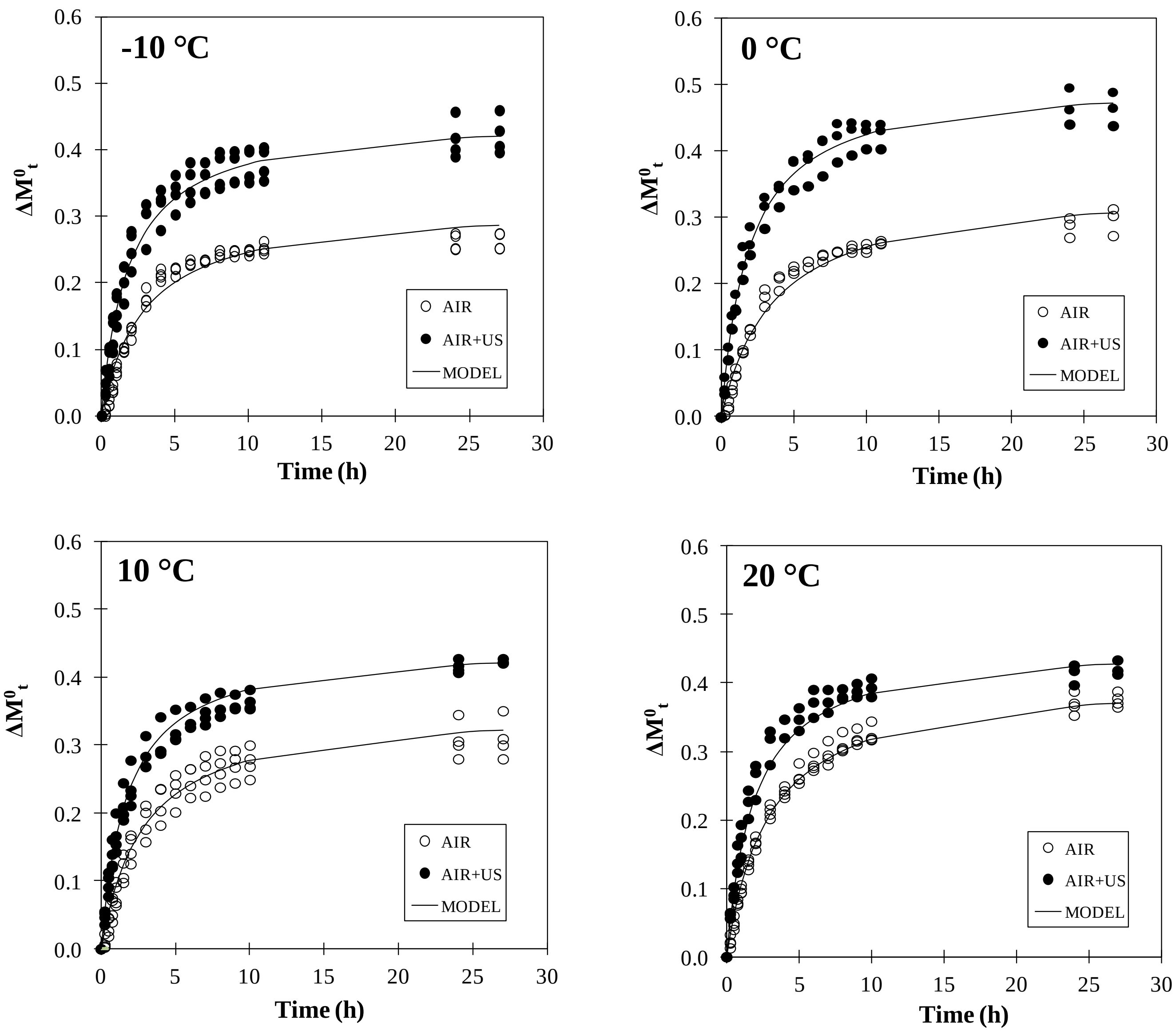

Figure 4

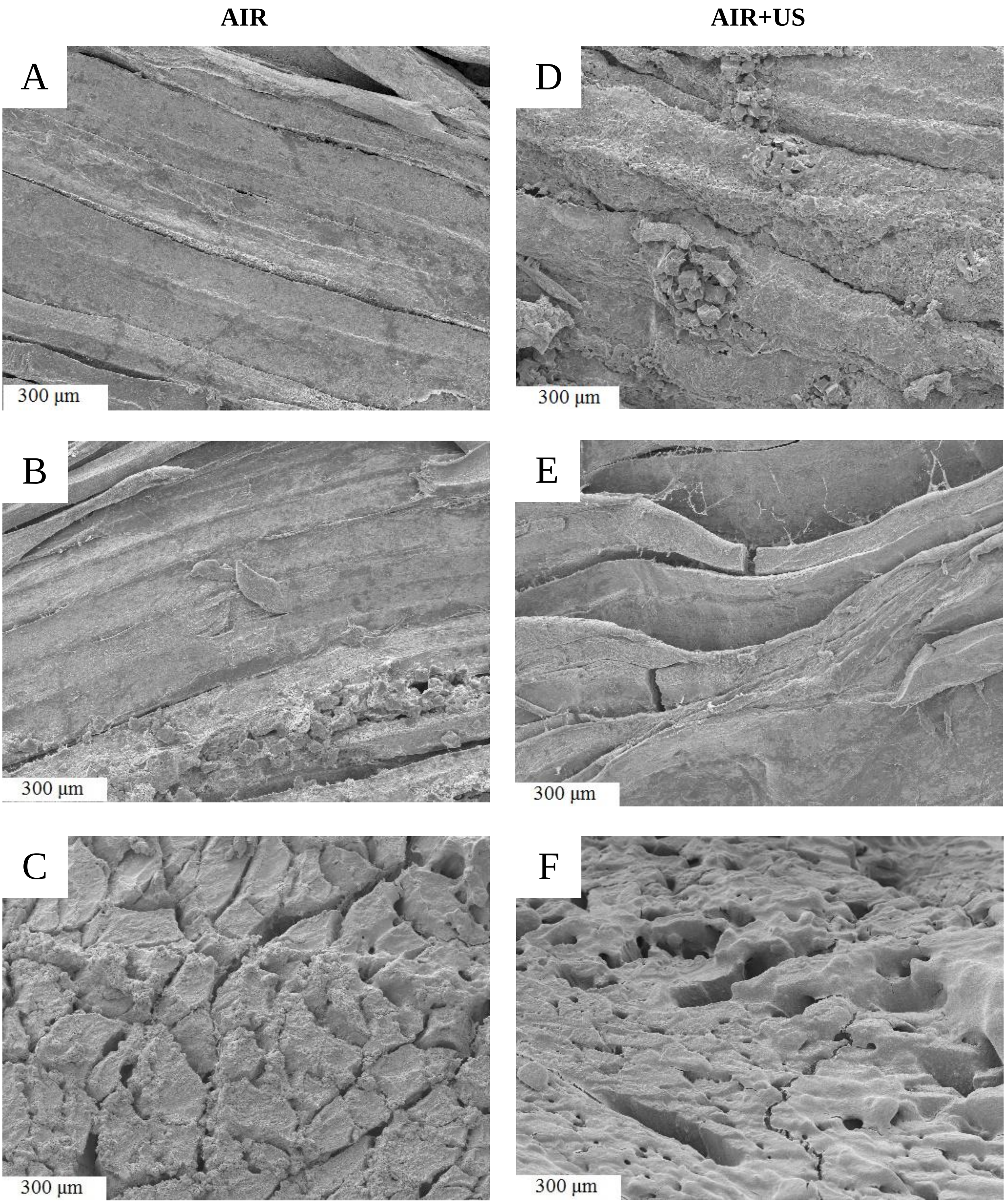

Figure 5

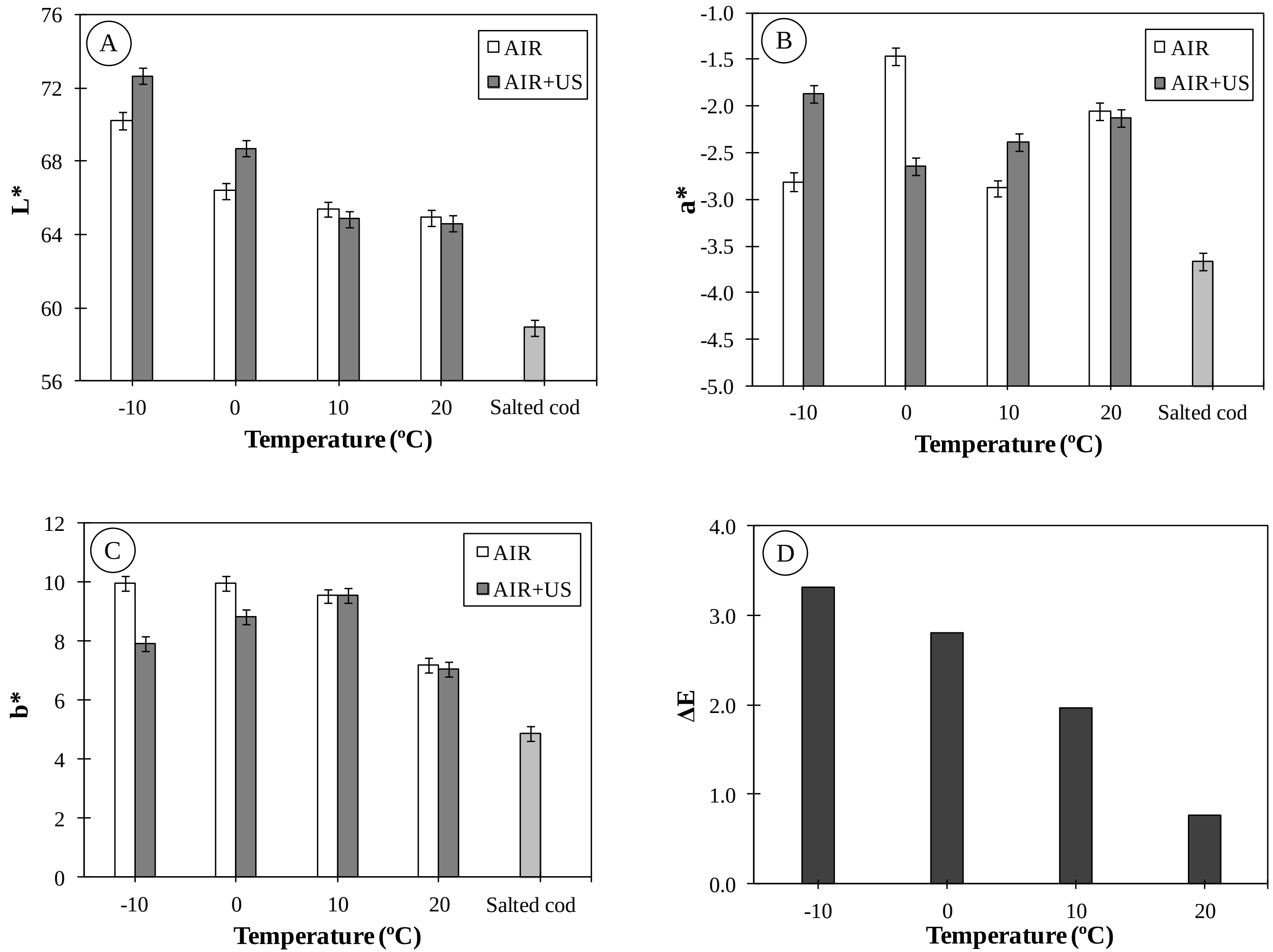
A
76
72
68
64
60
56
L*
AIR
AIR+US
-10
0
10
20
Salted cod
Temperature (ºC)
B
-1.0
-1.5
-2.0
-2.5
-3.0
-3.5
-4.0
-4.5
-5.0
a*
AIR
AIR+US
-10
0
10
20
Salted cod
Temperature (ºC)
C
12
10
8
6
4
2
0
b*
AIR
AIR+US
-10
0
10
20
Salted cod
Temperature (ºC)
D
4.0
3.0
2.0
1.0
0.0
ΔE
-10
0
10
20
Temperature (ºC)

Tables

Table 1. Average values and standard deviation of effective diffusivity, D_W, on salted cod drying. Increase in effective moisture diffusivity, ΔD_W (%), produced by ultrasound application and percentage of explained variance, VAR (%). The superscripts a, b, c, d and e show homogeneous groups established from LSD (least significance difference) intervals ($p<0.05$).

T (°C)		D_W (10^{-10} m^2/s)	VAR (%)	ΔD_W (%)
-10	AIR	$0.14 \pm 0.01_{a}$	98.3	-
	AIR+US	$0.25 \pm 0.02_{b}$	95.4	85.5
0	AIR	$0.21 \pm 0.02_{b}$	99.8	-
	AIR+US	$0.33 \pm 0.03_{c}$	99.6	57.3
10	AIR	$0.28 \pm 0.02_{b,c}$	99.6	-
	AIR+US	$0.40 \pm 0.04_{d}$	99.4	42.4
20	AIR	$0.35 \pm 0.01_{c,d}$	99.6	-
	AIR+US	$0.74 \pm 0.04_{e}$	99.9	110.1

Table 2. Experimental moisture and NaCl content of rehydrated (27 h) dried salted cod at -10, 0, 10 and 20 ºC with (20.5 kW/m^3, AIR+US) and without (AIR) ultrasound application. Average ± standard deviations are shown. The superscripts a, b and c (in moisture) and x (in NaCl) show homogeneous groups established from LSD (least significance difference) intervals ($p<0.05$).

T (ºC)		W (kg W/kg dry matter)	NaCl (kg NaCl/kg dry matter)
-10	AIR	$3.38 \pm 0.11_a$	$0.037 \pm 0.004_x$
	AIR+US	$3.80 \pm 0.20_c$	$0.036 \pm 0.004_x$
0	AIR	$3.37 \pm 0.19_a$	$0.041 \pm 0.005_x$
	AIR+US	$3.81 \pm 0.17_c$	$0.040 \pm 0.007_x$
10	AIR	$3.39 \pm 0.15_a$	$0.040 \pm 0.007_x$
	AIR+US	$3.76 \pm 0.12_c$	$0.040 \pm 0.005_x$
20	AIR	$3.00 \pm 0.13_b$	$0.040 \pm 0.009_x$
	AIR+US	$3.37 \pm 0.18_a$	$0.041 \pm 0.003_x$

Table 3. Modeling of the net weight gain, ΔM^0_t, by means of the Peleg model during rehydration of dried salted cod at -10, 0, 10 and 20 ºC with (20.5 kW/m^3, AIR+US) and without (AIR) ultrasound application. Increase in Peleg parameters, $\Delta 1/k_1$ and $\Delta 1/k_2$ (%), produced by ultrasound application and percentage of explained variance, VAR (%). The superscripts x and y (in $1/k_1$) and a, b, c, d and e (in $1/k_2$) show homogeneous groups established from LSD (least significance difference) intervals (p<0.05).

T (ºC)		$1/k_1$ (10^{-3} g W/g dry matter × s)	$1/k_2$ (g)	VAR (%)	$\Delta 1/k_1$ (%)	$\Delta 1/k_2$ (%)
-10	AIR	$1.8 \pm 0.2_x$	$0.32 \pm 0.01_a$	96.8	-	-
	AIR+US	$4.2 \pm 0.9_y$	$0.45 \pm 0.01_d$	98.8	133.0	41.8
0	AIR	$1.8 \pm 0.3_x$	$0.35 \pm 0.01_b$	97.7	-	-
	AIR+US	$4.4 \pm 0.4_y$	$0.51 \pm 0.02_e$	98.6	151.8	46.6
10	AIR	$2.2 \pm 0.3_x$	$0.36 \pm 0.02_b$	98.6	-	-
	AIR+US	$4.4 \pm 0.8_y$	$0.45 \pm 0.02_d$	99.3	104.1	25.8
20	AIR	$2.4 \pm 0.2_x$	$0.41 \pm 0.03_c$	98.7	-	-
	AIR+US	$4.1 \pm 0.7_y$	$0.46 \pm 0.03_d$	99.1	70.6	11.4

Table 4. Hardness (average ± standard deviations) of dried and dried+rehydrated-salted cod samples at -10, 0, 10 and 20 ºC with (20.5 kW/m^3, AIR+US) and without (AIR) ultrasound application. The superscripts a, b and c (in dried) and x, y and z (in dried+rehydrated) show homogeneous groups established from LSD (least significance difference) intervals ($p<0.05$).

T (°C)		Dried	Dried+Rehydrated
		Hardness (N)	Hardness (N)
-10	AIR	$9.93 \pm 0.80_a$	$1.13 \pm 0.13_x$
	AIR+US	$7.65 \pm 0.48_b$	$0.89 \pm 0.09_y$
0	AIR	$9.93 \pm 0.70_a$	$1.12 \pm 0.11_x$
	AIR+US	$7.30 \pm 0.61_b$	$0.88 \pm 0.10_y$
10	AIR	$11.58 \pm 0.50_c$	$1.17\pm 0.16_x$
	AIR+US	$7.31 \pm 0.55_b$	$0.88 \pm 0.10_y$
20	AIR	$12.4 \pm 0.96_c$	$2.38\pm 0.20_z$
	AIR+US	$8.25 \pm 0.57_b$	$1.19 \pm 0.17_x$